Rock and Soil Mechanics 2025 46(1): 110−122
https: //doi.org/10.26599/RSM.2024.94300350

ISSN 1000−7598
journal homepage: rocksoilmech.whrsm.ac.cn

Investigating pore characteristics and permeability of seasonally frozen turfy soil using multiple micro-test methods

HE Yuan-yuan[1, 2, 3], PENG Qi-lan[1, 2, 3], WANG Li[1, 2, 3], WANG Shi-mei[1, 2, 3], NIE Lei[4], XU Yan[4], LÜ Yan[4], CHEN Yong [1, 2, 3], ZHANG Xian-wei[5]

1. Key Laboratory of Geological Hazards on Three Gorges Reservoir Area, Ministry of Education, China Three Gorges University, Yichang, Hubei 443002, China;

2. Hubei Key Laboratory of Disaster Prevention and Mitigation, China Three Gorges University, Yichang 443002, China

3. College of Civil Engineering & Architecture, China Three Gorges University, Yichang 443002, China

4. College of Construction Engineering, Jilin University, Changchun, Jilin 130026, China;

5. State Key Laboratory of Geomechanics and Geotechnical Engineering, Institute of Rock and Soil Mechanics, Chinese Academy of Sciences, Wuhan, 430071, China

Abstract: The macroscopic properties of soil are mainly affected by its microstructure and pore characteristics. To figure out the microscopic evolution of soil under the influence of external conditions such as freeze-thaw is significant for geotechnical study. As seasonally frozen and special soil, turfy soil has high compressibility and low strength due to its high humus and plant fiber content. Thus, this study took turfy soil to investigate its microstructures, pore characteristics, and effect of freeze-thaw by methods including geotechnical tests, nuclear magnetic resonance (NMR), X-ray Computed tomography (CT), and scanning electron microscope (SEM). Based on geotechnical and NMR theory, micro-image segmentation was completed on CT slices and SEM images to identify air and water-storage pores. Combined with microscopic images and composition analysis, the microstructure of turfy soil reveals that the organic matter component is the soil matrix able to contain and conduct water. The pore size distribution of turfy soil after freeze-thaw showed an increase in the proportion of mesopores and a significant increase in the number of pores. Consequently, the quantitative characterization of microscopic parameters indicates that the pore connectivity of turfy soil before and after freeze-thaw is enhanced, and the complexity of the pore shape is reduced, enhancing permeability. Finally, verifying the theoretical calculation of unsaturated soil shows that the NMR method can effectively characterize the change in permeability of freezing and thawing soil. This work can serve as the basis of studies on soil with high organic matter and high fiber content and can be applied as a parameter basis for engineering construction in turfy soil distributed regions.

Keywords: Turfy soil; Freeze-thaw; Microstructures; Pore characteristic; NMR; CT

1 Introduction

Soil is a multiple-phase system containing mainly air, water (ice, when freezing), and soil grains, in which soil skeletons and pores constitute the main structure. Particle and pore size distribution are key parameters to describe soil structure, which can be applied for soil classification and determination of soil permeability with a wide range of applications in civil engineering, agriculture, forestry, and environmental science. Pore characteristics greatly influence soil mechanisms and fundamental physical properties, which are essential to determining moisture migration and solute transport within the soil. Generally, pore characteristics of soil change under freeze-thaw, dry-wet process, and the action of other forces, resulting in significant strengthening or deterioration of soil properties and mechanical strength[1; 2]. It greatly influences frozen soil's water and heat distribution [3; 4]. Thus, the fine quantification and microscopic visualization of soil pore characteristics is of great significance to the study of soil mechanics and soil science.

Nitrogen adsorption (NA) and mercury intrusion porosimetry (MIP) are the most commonly used traditional methods to determine soil pore size distribution and specific surface area. These methods are based on physical or chemical principles and have the advantages of good operability and high accuracy of measurement results. Still, they also have the disadvantages of time-consuming, expensive, or disturbing the sample[5]. The nitrogen adsorption method can give accurate results of sample micropore (nm level) determination, but there are some errors in larger pore (μm level) size determination. Besides, the mercury intrusion method determines soil pore size by the relationship between the amount of mercury intake and the pressure. When measuring the pore size of micropores, excessive pressure will damage the sample

Received: 24 February 2024 Revised: 10 September 2024
This work was supported by the Open Fund of the Key Laboratory of Geological Hazards on Three Gorges Reservoir Area (China Three Gorges University), Ministry of Education (No. 2023KDZ10), Youth Fund of Hubei Natural Science Foundation (No. 2024AFB082), National Natural Science Foundation of China (Grant No. 41702300, Grant No.41572254) and the Open Fund of Hubei Key Laboratory of Disaster Prevention and Mitigation (No.2023KJZ23).
First author: He Yuan-yuan, male, born in 1996, PhD, focusing on special soil and soil microstructures. E-mail: heyuanyuan@ctgu.edu.cn
Corresponding author: Wang Li, male, born in 1988, PhD, focusing on Geological disaster prediction and evaluation. E-mail: wangli_ctgu@126.com

structure on one hand and will also cause deviations in the measurement results of the micropore diameter. New techniques, such as X-ray Computed tomography (CT), scanning electron microscope (SEM), and nuclear magnetic resonance (NMR) and numerical simulation, are gradually applied to investigate microstructures, pore characteristics of soil, with advantages of 2D, 3D visualization, 3D reconstruction, and seepage analysis[6-8]. The soil pore size distribution obtained by SEM, CT images and NMR T_2 spectra greatly depends on how the image segmentation threshold and surface relaxivity are determined, closely related to soil type, clay content, organic matter content and other soil properties[9-11]. Many researchers have applied two or more combined approaches to explore soil pore size distribution and to compare the applicability and accuracy of different methods. Yang et al. [12]used CT combined MIP to identify pores with 18 – 344μm diameter, which is the overlapping pore range by the 2 methods, and a suggested threshold for CT segmentation was proposed. Zong et al. [13]applied MIP, NA and CT to describe the pore size distribution of 4 different soils. This indicates that the combined method can quantify soil PSD over a wider range and be verified and calibrated mutually. Jia et al. revealed the evolution of pore structures influenced under frost damage by NMR measurements in combination with SEM, which was reflected in micro-parameters and hydrological parameters, including porosity, pore size distribution, permeability, tortuosity, and pore non-uniformity[14].

The soil freezes and thaws cyclically in seasonally frozen regions, with an atmospheric temperature rising and falling periodically. Synthetically, water-ice phase change, pore water migration, and frost damage drive the pore characteristics and permeability of the soil to change greatly, macroscopically reflected as frost heave and thaw settlement[15-17]. Variation of pore size distribution, fractal dimension, connectivity, and other pore characteristics after freeze-thaw is influenced by external factors (freeze-thaw cycles, temperature, and load) and internal factors (rock and soil type, water content, and degree of compaction)[18-20]. Consequently, it is significant to figure out pore characteristics of special soil distributed in seasonally frozen regions, which can serve as a parameter basis for soil hydraulic properties, engineering construction and agricultural utilization. Turfy soil is a high organic matter content humus soil consisting of plenty of plant fibers and decomposed humus, widely distributed in the high-altitude and high-latitude cold regions, including the Greater and Lesser Xing 'an Mountains, Changbai Mountains, Ruoergai Plateau in Western Sichuan, and the mountainous areas in northern Xinjiang, et al. The low-lying terrain, water-rich stratum environment, lush surface vegetation, and cold long winter provide a good natural environment for the formation of turfy soil[21]. In detail, the decomposition environment of a water-rich and anoxic soil layer makes the decomposition of plant residues slow and incomplete, and the plant fibers in turfy soil are crisscrossed, which is different from common peat soil[21]. The vegetation grows and dies repeatedly in the seasonally frozen turfy swamps, and the organic matter accumulates and decomposes continuously, which makes turfy soil have the characteristics of high organic matter and high plant fiber content. Meanwhile, studies have shown that turfy soil has poor engineering geological properties, such as high compressibility and low strength[22; 23]. Interlaced plant fibers form a skeleton, making the soil structure loose, with high permeability, porosity, and water content. Therefore, the investigation of pore characteristics and microstructure is a key point to studying the properties of turfy soil, which can provide a theoretical basis for engineering construction, agricultural utilization, and ecological environmental protection in seasonally frozen turfy swamps.

This study compared pore characteristics of turfy soil obtained by SEM, CT, and NMR, based on 2D and 3D visual perspective and NMR theoretical derivation. Furthermore, temperature-controlled NMR measurements were conducted to investigate pore structures varying during the freeze-thaw process, revealing the influences of phase change and pore water immigration on soil microstructures and pore characteristics. Micro-parameters, pore characteristics and hydraulic properties were analyzed in conjunction with soil properties to gain a deeper understanding of the structure of turfy soil. In addition, the permeability of freezing and thawing turfy soil was derived based on pore characteristics, which can serve as a parameter basis of hydrothermal coupling and seepage analysis. Overall, it is expected that this work can serve as a sound theoretical and experimental experience for soil microstructures and pore characteristics, especially for high-organic matter humus soil distributed in cold regions.

2 Materials and method

2.1 Study area and soil samples

Turfy soil in this study was sampled at a low-lying wetland near National Highway 201 and the Heda Expressway in Jiangyuan Town, Dunhua, Jilin Province, China, which belongs to the Changbai Mountain System which is a typically seasonal frozen region, as shown in Fig. 2. The sampling point area belongs to the monsoon climate of medium latitudes, which brings abundant rainfall, and long and cold winters, and provides good climatic conditions for the formation of turfy swamps. The extreme value of minimum temperature is -35.78 ℃, the extreme value of maximum temperature is 36.39 ℃, the annual average temperature is 4.07 ℃, the average temperature in summer is 19.60 ℃ and the average temperature in winter is -13.15 ℃. About 140 days of daily average temperature is lower than 0 ℃, and about 195 days of minimum temperature is lower than 0 ℃ (data source: literature[24]).

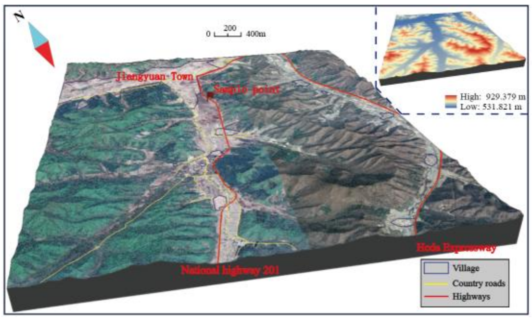

Fig.1 Geographical location, topography and surrounding roads of sampling point

Sampling time was in October before the winter and after the rainy season, and turfy swamps were not waterlogged, making it easier to take samples. The depth of the turfy soil layer at this point is 1.6m, and the underground water level is 1.75m. The sampling process is as follows: 1) Using shovels to remove surface vegetation, a 1.5 m×1.5 m square surface was opened up; 2) Using a 20 cm thin-walled extractor to continuously static pressure into the soil; 3) then extracting the soil sample, encapsulating the soil sample with wax seal at both ends to prevent water evaporation; (4) marking the soil sample up and down, and using the black plastic bag cover as a light-proof treatment ; (5) repeating step (1), continue to sample downward and flatten the layer after sampling each layer until the sampling reaches the underlying stratum of turfy soil.

2.2 Test methods for fundamental properties of turfy soil

Turfy soil has a high organic matter content; thus, determining fundamental properties differs slightly from other common soil. In detail, the oven drying temperature is adjusted to 60℃ to prevent loss of organic matter. The medium of the kerosene pycnometer method is anhydrous kerosene instead of water, which can sink the organic matter components. The decomposition degree is a significant index quantifying how many plant fibers decomposed within turfy soil, and the detailed determination method is referred to in He's study[24]. Determining fundamental properties on turfy soil referred to the Standard for geotechnical testing method[25], listed in Table 1. Consequently, the properties of turfy soil from different layers are shown in Table 2. According to the particle size classification system of the Food and Agriculture Organization of the United Nations (FAO) and the United States Department of Agriculture (USDA), soil particles with a size of less than 0.002 mm are classified as clay, particles ranging from 0.002 to 0.05 mm are classified as silt, and particles larger than 0.05 mm are classified as sand. Thus, C_{clay} and C_{silt} are clay and silt content of turfy soil.

Table 1 Test method to determining fundamental properties of turfy soil

Property	Method
Water content (ω)	Oven drying method (60 ℃)
Natural density (ρ_b)	Cutting-ring method
Specific gravity (ρ_s)	Kerosene pycnometer method
Particle distribution	Laser particle size analyzer (BT-9300LD, China)
Organic matter content (O_c)	Loss on ignition method (450 ℃)
Decomposition degree (D_d)	NaOH solution boiling method
Permeability coefficient (K_ω)	Variable head permeability test

2.3 Micro-test methods

Nuclear magnetic resonance (NMR) is an effective method to measure pore water content and microstructures of porous materials. It is now widely used in geotechnical and energy fields, especially for soil and rock pore characteristics studies. The presence of H atoms in soil pore water makes the content of soil pore water and the occurrence of environmental information can be easily determined by the NMR method. This study used 23.1 MHz NMR equipment developed by Suzhou Niumag Analytical Instrument Corporation, China, consisting of a magnet unit, sample tube, NMR measurement system, and data collection system (Fig.2). For continuous measurement during the freeze-thaw process, a refrigeration cycle and temperature controller are installed outside NMR equipment, and the temperature control range was -40 ℃ to 99 ℃ with an accuracy of 0.1 ℃. The soil sample is cooled with a water-free fluoride solution, which does not cause signal interference to the NMR

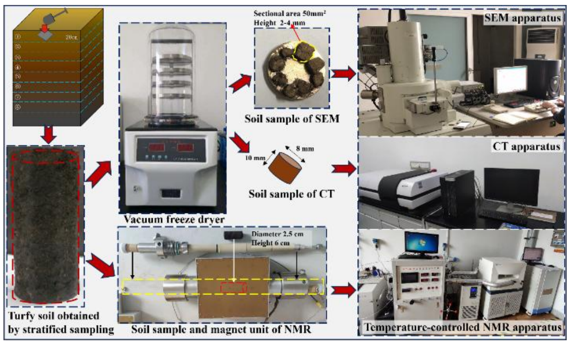

Fig.2 Microscopic measurement process diagram

Table 2. Fundamental properties of turfy soil from different layers

Layer	ω /%	ρ_b /(g・cm^{-3})	ρ_s /(g・cm^{-3})	K_w/(cm・s^{-1})	O_c /%	D_d/%	C_{clay} /%	C_{silt} /%
1	154.06	1.090	1.901	8.07×10^{-5}	39.158	62.635	1.72	67.82
2	165.14	1.030	1.879	4.07×10^{-5}	49.563	58.804	1.64	65.54
3	161.03	1.131	1.617	7.88×10^{-5}	41.496	85.478	2.09	66.92
4	253.31	1.100	1.457	9.12×10^{-5}	72.036	91.264	0.91	51.38
5	290.73	1.029	1.532	3.82×10^{-5}	80.244	92.599	0.92	54.15
6	297.61	1.035	1.495	8.94×10^{-5}	76.766	88.715	0.90	52.48
7	259.25	1.072	1.490	2.22×10^{-4}	75.334	94.955	0.66	48.31
8	225.34	0.954	1.487	3.86×10^{-4}	79.793	93.080	0.77	51.16

measurement. Meanwhile, the fluoride solution is cooled to the set temperature by a cold bath machine with anhydrous ethanol as the circulating refrigeration liquid. The measurement procedure can be divided as follows: (1) turfy soil is treated as a 2.5 cm diameter, 6 cm height cylinder and put in the sample tube; (2) soil is cooled or warmed to the set temperature and held for at least 1 h, while the temperature of the sample is monitored and controlled by sensors in the sample tube and cold bath equipment; (3) NMR measurement is conducted at each temperature every 20 minutes using Carr-Purcell-Meiboom-Gill (CPMG) sequence[26; 27], and stopped when the error of three consecutive measurements does not exceed 2 %. Besides, results are calibrated to reduce the influence of temperature on NMR intensity by Curie's law and related NMR research[28].

Furthermore, microstructures and pore characteristics of turfy soil were measured by the SEM, CT and NMR methods (Fig. 2). The undisturbed samples of turfy soil were cut into specified shapes for SEM and CT measurements. Then the same samples were used for specimen preparation after experiencing a freeze-thaw process. In particular, the freezing temperature is 0–-15 ℃ at each integer point, and each temperature point is kept for 2h. The thawing temperature is 5 − -15 ℃at each integer point, and each temperature point is kept for 2h, the same as the process of NMR measurements. Secondly, the prepared samples were freeze-dried using the vacuum liquid nitrogen freezing method, which was more able to retain the integrity of the soil structure than the oven drying method. Finally, SEM and CT methods can obtain micro-images of turfy soil. The SEM instrument in this study is a JSM-6700F scanning electron microscope produced in Japan, which can be used to obtain images with a magnification of 650,000 times. The CT instrument is the Skyscan 1172 desktop X-ray CT system produced by Bruker Microct, Belgium, with a maximum resolution of 0.5 μm / pixel.

2.4 Background theory

(1) Theory of geomechanics

Soil porosity is an important index to reflect the degree of soil looseness, and it is an indispensable parameter basis in the process of engineering construction, agricultural farming and resource development. Traditionally, the soil porosity can be calculated by the experimental results of fundamental physical properties, as follows:

$$n_{\text{Cal}} = 1 - \frac{\rho_d}{\rho_s} \times 100\% \qquad (1)$$

where ρ_d and ρ_s are the dry density and specific gravity of soil.

The permeability of frozen soil varies continuously with the degree of freezing and thawing, which is closely related to the liquid water content and soil texture. The theoretical approaches (VG model) for calculating soil hydraulic properties proposed by Van Genuchten [29] and Mualem [30] are introduced to calculate the permeability of turfy soils during freeze-thaw as follows:

$$K_{\text{VG}} = K_s S_r^l \left[1 - (1 - S_r^{1/m})^m\right]^2 \qquad (2)$$

where K_{VG} is the permeability coefficient of water in the soil is calculated by the VG model, S is the water saturation of the soil, K_s is the saturated permeability of soil and l, m are the empirical parameters related to soil texture, which are respectively 0.5 and 0.22 for turfy soil according to soil classification[31; 32].

(2) Micro-images processing

Pore size distribution of soil is similar to particle size distribution, and they both are highly related to sedimentation, strength, water-holding and water-conducting capacity of soil. From CT and SEM micro-images, professional image processing and data statistics can identify pore size distribution. Referred to related studies on identifying pores in soil micro-images by determination of segment threshold[33-35], this study adopted 60–90 as the threshold value of micro-image combined watershed segmentation to divide pores from turfy soil. After basic image processing, pore characteristics parameters, including radius, area, fractal dimension, perimeter, axis angle, and other shape factors, can be obtained for further analysis.

Based on the pore connectivity, permeability in soil (k_ω) can be further calculated by CT 3D reconstruction of soil samples, and the permeability coefficient of water in soil (K_ω) can be derived by conversion relationship. The conversion relationship between k_ω and the permeability coefficient K_{ω} obtained by the variable head experiment is as follows,

$$K_{\omega} = k_{\omega}\rho_{l} g / \eta \quad (3)$$

where, ρ_l is the fluid density, g/cm^3, g is the acceleration of gravity, m/s^2, and η is the dynamic viscosity coefficient, Pa·s.

(3) NMR theory and size information of porous media

NMR T_2 is the transverse relaxation time, including most of the physical information of the porous medium, and it is an extremely critical goal for NMR measurements. After each measurement, the T_2 distribution curve can be obtained by echo string inversion processing technique, and the signal intensity characterizes the pore characteristics of the porous medium and the liquid water content. Ice, as a solid material, is another phase of water, and its transverse relaxation time during NMR measurements is very short (T_2 < 5μs), which is very different from that of liquid water. Therefore, the relaxation process of ice occurs during the dead time of the NMR system measurement and is undetectable. In contrast, the lateral relaxation time T_2 of liquid water in porous media materials measured by NMR highly depends on pore characteristics. The magnitude of T_2 reflects the size of the pores in which the liquid water is located. Based on this feature, the liquid water content and pore size distribution of soil can be determined by NMR method, and the soil liquid water at negative temperature is the unfrozen water in the frozen soil. In saturated soil, pores can be seen as filled with water. Thus, the porosity of saturated soil is positively correlated to pore water content. Turfy soil is distributed in the water-rich swamp environment with a high water content. Therefore, undisturbed soil samples in this study can be regarded as saturated, and pore characteristics can be analyzed by NMR T_2 distribution.

The peak area of the T_2 distribution represents the total signal intensity of the liquid water inside the soil, and T_2 contains pore information as follows,

$$\frac{1}{T_2} = \frac{1}{T_{2\mathrm{Bulk}}} + \frac{1}{T_{2\mathrm{Surface}}} + \frac{1}{T_{2\mathrm{Diffusion}}} \quad (4)$$

where $T_{2\mathrm{Bulk}}$ is the bulk relaxation time, $T_{2\mathrm{Surface}}$ is the surface relaxation time and $T_{2\mathrm{Diffusion}}$ is the diffusion relaxation time. $T_{2\mathrm{Bulk}}$ indicates the relaxation time of a pore fluid measured in a sufficiently large vessel (the effect of the vessel is negligible), $T_{2\mathrm{Surface}}$ indicates the pore fluid relaxation time by the solid-liquid interface, and $T_{2\mathrm{Diffusion}}$ indicates the relaxation time of pore fluids induced by diffusion in a gradient in the static magnetic field. The research illustrated that $T_{2\mathrm{Bulk}}$ is much larger than $T_{2\mathrm{Surface}}$ and $T_{2\mathrm{Diffusion}}$, and its effect on 1/ T_2 is inappreciable[36]. Besides, for porous media, especially soil, which belongs to a fast-diffusion regime, $1/T_{2\mathrm{Diffusion}}$ on T_2 is also negligible[37]. Thus, Equation (4) can now be simplified as,

$$\frac{1}{T_2} \approx \frac{1}{T_{2\mathrm{Surface}}} = \rho\left(\frac{S}{V}\right) = \rho\left(\frac{F}{R}\right) \quad (5)$$

where ρ is the surface relaxivity of soil related to pore wall composition, roughness and soil clay, organic matter content[9; 11], *(S/V)* is the ratio of surface area to pore volume which is inversely proportional to pore radius, R is the radius of the pore, F is a factor controlled by pore shape geometry which usually takes 1, 2, 3 corresponding to planar, cylindrical and spherical pores, respectively. There are many studies aiming to quantify surface relaxivity (ρ) of materials of rock and soil by NMR method combined soil water retention curves (SWRCs) or mercury intrusion porosimetry (MIP) test, which can be directly used to describe pore size distribution for high resolution, especially in nm-range. Jaeger compared conventional methods (SWRCs) and NMR for measuring the pore size distribution of 6 disturbed soil samples with various textures and organic matter content[38]. Results show that the average ρ can estimate soil pore size distribution by the NMR method quickly and non-destructively. Meyer determined ρ for the macropore and medium pore of 7 different soils by WRC calibration[39]. One type in these soils has a similar particle size distribution to turfy soil and relatively high organic matter content. In detail, a silty loam in Jaeger's research contains 23.0 % clay grains, 52.0 % silt grains, 25.0 % sand grains, and natural density (1.17 g/cm^3), which is close to the properties of turfy soil. Thus, the average ρ of turfy soil takes 35 μm/s for estimating pore size distribution.

Referred to the porosity of sandstone derived by the NMR method[14], the porosity can be calculated as follows,

$$n_{\mathrm{NMR}} = \frac{M_{0(\mathrm{ts})}}{M_{0(\omega)}} \quad (6)$$

where $M_{0(\mathrm{ts})}$ is the NMR signal magnitude measured for turfy soil at different temperatures, and $M_{0(\omega)}$ is the NMR signal magnitude of pure water of the same size as soil samples under the same measuring conditions.

The permeability coefficient(K_{NMR}) can be obtained by NMR method, which is derived from the prediction model proposed by Coates et al.[40], based on the bulk water / bound water ratio, as follows,

$$K_{\mathrm{NMR}} = 10^{-11} n_{\mathrm{NMR}}^{4} \left(\frac{\mathrm{BVI}}{\mathrm{FFI}}\right)^{2} \quad (7)$$

where BVI and FFI are the bound water and bulk water content, respectively. Soil pore water division was based on previous research results[41].

3 Results and discussion

3.1 Visual microstructure of turfy soil

Generally, micro-images obtained by SEM and CT methods must be pre-treated, including enhancement, noise reduction, shadow elimination, and other image-processing steps. In this study, the software equipped by the instrument manufacturer was used for ring shadow elimination, noise reduction, and image enhancement. The FDK algorithm converted the projected image into a 2D CT image[42]. Through the image's obvious grey difference and component contour, the various substances and structures in the soil can be seen only by the naked eye.

In SEM images, microstructures of turfy soil show laminated characteristics, and soil is relatively loose with many pores distributed (Fig. 3). Especially the structure of plant residues, including vessels, sieve tubes, and rhizomes, occupies a large part of the soil. Turfy soil comprises most plant residues and a small amount of soil matrix and mineral layered extrusion together, and the soil matrix is attached to the plant residues. The pores are divided into small pores between different components, and large pores are distributed along plant fibers. The shape of small pores is closely related to the morphology of soil particles and the distribution of plant residues. Macropores are mainly extended along the distribution direction of plant residues, indicating that plant residues form an overhead structure as a skeleton in turfy soil. In addition, obvious sieve-like ducts, which are natural water passages, can be seen. The high-magnification electron microscope image shows that the proportion of pores in the soil is high, and the shape is extremely irregular. The minerals in the turfy soil are mainly montmorillonite and a small amount of kaolinite, and the particle morphology shows flake and flocculent. Most soil particles are point contact, with linear contact between plant residues and soil particles. Decomposed organic matter is distributed in extremely irregular forms between soil particles and plant residues, forming a bonding structure.

Results obtained by CT are thousands of slice sequences, and the CT image segmentation threshold of turfy soil is determined based on the calibration of turfy soil's physical properties[43]. A single slice can be used to explain the microstructure and pore characteristics of a plane in the soil, and sequence combination can be used for three-dimensional reconstruction (Fig. 4). That is, the CT method expands 3D visualization, which can get more information on soil microstructures from multidimensional with fixed resolution. The most prominent bright spot in the CT image is mineral particles, the black part is air pores, and the main grey part between the two is organic matter. Based on this criterion, thresholds can be set for each component in the turfy soil to complete the image segmentation. To optimize the effect of image segmentation, the most widely used image segmentation algorithm, namely the watershed algorithm, is adopted[44]. As shown in slice segmentation and 3D reconstruction, organic matter is the main component in turfy soil, forming the matrix. The hollow pores are distributed along the plant fibers, and the mineral particles are dotted embellishments attached to the matrix. In contrast, SEM can better show the details of the microstructure and pore characteristics of the soil, including particle morphology, component contact characteristics, and structural characteristics. CT focuses more on the complete display of the overall structure of the soil. By combining with the SEM and CT results, it can be concluded that turfy soil has microstructures of organic matter fractions as the matrix, plant fibers as the skeleton, mineral particles distributed and hollow pores contained therein.

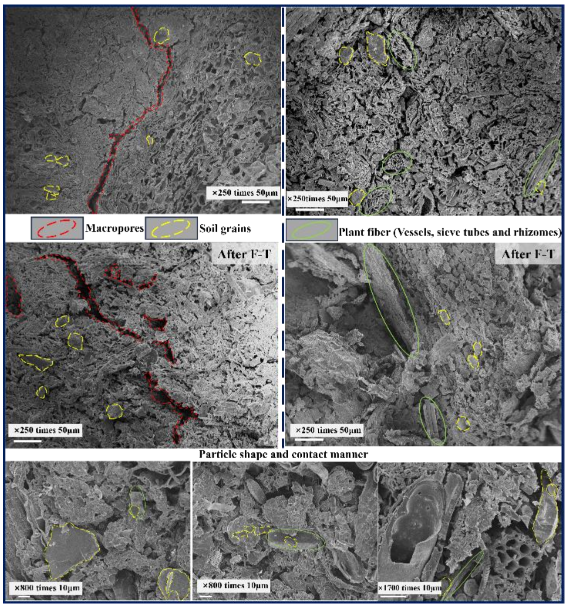

Fig.3 Microstructure and pore characteristics of turfy soil before and after F-T obtained by SEM

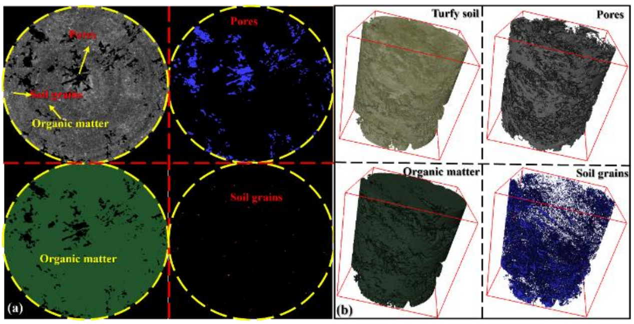

Fig.4 Microstructure and 3D reconstruction of turfy soil obtained by CT (a. The segmentation of each component by the watershed algorithm; b. 3D reconstruction of each component)

3.2 Quantification of soil microstructures effects of freeze-thaw on pore characteristics

3.2.1 Porosity

As shown in Fig. 5, the segmentation of the micro-image illustrates a comparison of turfy soil from layers 3 and 5 before and after freeze-thaw. After a freezing-thawing process, the soil undergoes a water-ice phase transition and ice-thawing process. The difference in the density of water and ice will cause about 10 % volume expansion, and this part of the expansion volume will be restored after the ice melts[41]. Therefore, the ice formation will form new small pores in the soil and connect the original pores, generating microscopic cracks. The microscopic parameters can quantitatively express the changes in soil after freeze-thaw.

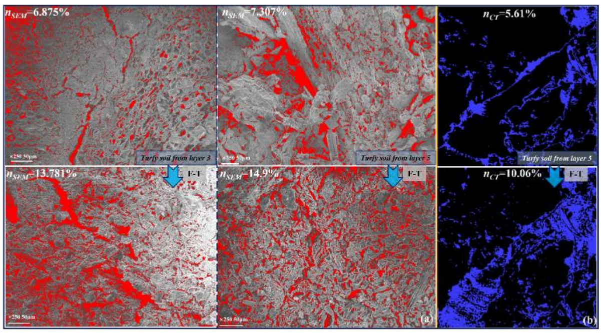

Fig.5 Pores within turfy soil before and after F-T identification (a. SEM images; b. CT slice)

The parametric quantitative expression of pore characteristics and microstructure is an effective way to help us better reveal and compare soil composition, component morphology and hydraulic properties. Porosity (n) is the percentage of pore volume in the soil to the total volume, which is an important parameter to express the compactness of the soil. By micro-image segmentation, pores can be identified exactly in soil, and its 2D-plane shape factor (area, perimeter, fractal dimension, etc.) and 3D-shape information (volume, surface area) can be derived from SEM images and CT slices, respectively. Table 3 and Fig. 6 listed porosity and organic matter volume ratio (V_{Oc}) obtained by micro-image segmentation statistics, theoretical calculation of geotechnics and results of fundamental properties determination (Eq.1) and NMR method (Eq. 6).

Why does porosity derived by different methods vary greatly, especially between image segmentation (n_{SEM} and n_{CT}) and theoretical calculation (n_{Cal} and n_{NMR})? The porosity of turfy soil is about 10 % in image recognition, while the theoretical calculation results reach 60 − 80 %.

Table 3 Porosity of turfy soil obtained by SEM and CT segmentation

	n_{SEM} /%		n_{CT} /%	V_{Oc} /%
Soil layer	3	5	5	5
Before F-T	6.88	7.31	5.61	92.58
After F-T	13.78	14.90	10.06	88.45

Note: n_{SEM} is the porosity obtained by SEM image segmentation, n_{CT} is the porosity obtained by CT 3D reconstruction combined with the watershed algorithm, and V_{Oc} is the volume ratio of organic matter.

In this case, it is important to emphasize that the split and reconstructed pores are air pores. In conjunction with Fig. 7, it can be seen that Equation (1) indicated that the porosity n_{Cal} is a function of the ratio of the dry density of turfy soil (ρ_d) to the density of the particles (ρ_s). The density of mineral particles (about 2.65 g/cm^3 for quartz and 2.8 g/cm^3 for clay particles) is much higher than the density of organic matter (only 0.2−0.5 g/cm^3 for dry wood and even lower for grassroots and humus) in turfy soil. Moreover, the main controlling factors of the particle density of turfy soil are minerals and humus. The dry density of turfy soil is extremely low (0.26−0.433 g/cm^3) because of the high ratio of organic matter fractions (Mean content: 64.30 %). Therefore, the porosity n_{Cal} considers the organic matter fraction in turfy soil as pores. Combined with Fig. 5, it can be concluded that the organic matter has a property similar to the "foam". That is, the organic matter in turfy soil has extremely low-density characteristics; meanwhile, it can absorb and contain water. However, there is also a pure "air pore" component, which can be identified by micro-image grey segmentation, the space within turfy soil that is without minerals and organic matter, and this inference is consistent with the research of Gong[45]. Similarly, the porosity n_{NMR} calculated by the NMR method is the volume ratio of all available water storage spaces, which is also much larger than the air porosity.

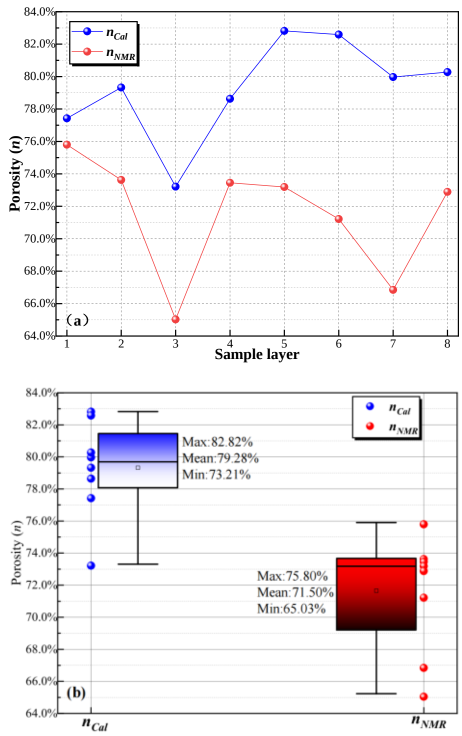

Fig.6 Porosity of turfy soil obtained by theoretical calculation (a. by geotechnics and results of fundamental properties determination; b. by NMR method)

3.2.2 Pore size distribution

Since the thickness of the specimen characterized by each image obtained from CT scanning is the same, the purpose of comparison can be achieved by selecting the same number of images in the sequence of CT scanning tomography images of the same sample. The CT scanning tomography images of turfy soil from layer 5 at roughly the same level before and after freeze-thaw were selected, and the image segmentation of air pores was carried out separately. The changes in the distribution of air pores can be obtained as shown in Fig. 8. By comparison, the naked eye can identify that the distribution of air pores in turfy soil after freeze-thaw becomes wider, and some of the original air pore area expands outward to form larger air pores. Besides, some isolated air pores are connected, forming more small pores. The phenomenon observed by comparing the CT scan tomography images is consistent with the conclusion of the NMR-based unfrozen water determination test in He's study (16). This comparison can be quantified by the number, volume, surface area, and effective radius of air pores, as shown in Fig. 8.

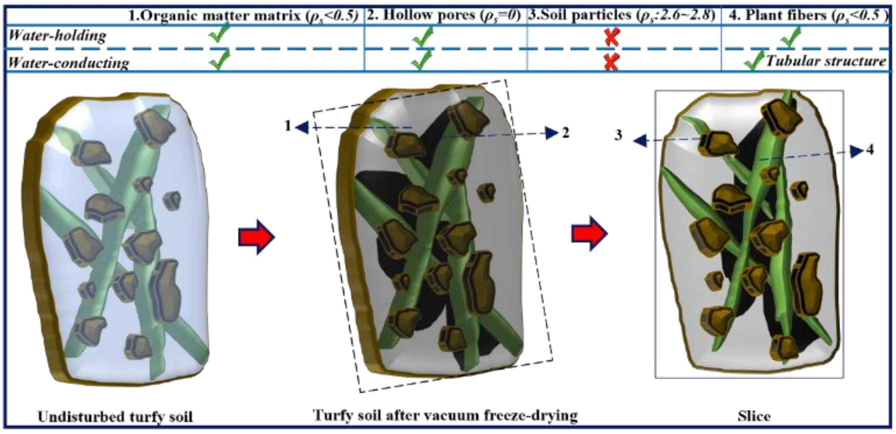

Fig.7 A schematic diagram of the microstructure and characteristics of each component of turfy soil

According to the Soil Society of America's soil pore classification criteria based on pore size, i.e., pore effective radius <0.05μm for cryptic pores, 0.01 to 2.5μm for ultramicro-pores, 2.5 to 15μm for micropores, 15 to 40μm for mesopores, and greater than 40μm for macropores. In this study, the pore space of turfy soil was categorized as macropores, mesopores, and micropores, defined as effective radius >40μm, (>15, ≤ 40 μm), and <15μm, respectively. It can be seen that the number of micropores (mean radius: about 10μm) and mesopores (mean radius: about 24μm) in turfy soil is the largest, accounting for the highest proportion, which is inferred as soil particle gap and soil particle and plant residue gap. The macropores (mean radius: about 59 μm) are mainly through pores distributed along plant fibers. Contrastively, the number of isolated air pores of turfy soil after freeze-thaw increases substantially, especially the number of mesopores, which is increased most obviously, followed by large and small pores. Regarding ratio variation, the percentage of mesopores and macropores increases after freeze-thaw while the percentage of macropores decreases.

The results of SEM image segmentation are shown in Fig. 9; the cumulative curve indicated a trend similar to CT results. However, the size of air pores in turfy soil obtained by SEM (Mean radius: 2−3μm) is far smaller than the results of CT (about 20μm). The pore size distribution results of CT are based on the statistics of 3D reconstruction, which is the analysis of the three-dimensional pore size distribution of soil. Therefore, in the longitudinal direction, which is also the most densely distributed direction of roots in turfy soil, the volume of air pores is larger, which is also unrecognizable by surface scanning SEM. At the same time, limited by the resolution, pores of 1μm level are difficult to identify in CT. SEM can be enlarged to tens or even hundreds of thousands of times, and micropores of 0.1μm level can also be identified. In general, these two methods have their advantages in soil microscopic identification. SEM can obtain more accurate soil surface microstructure, and CT can investigate the overall pore distribution of the sample.

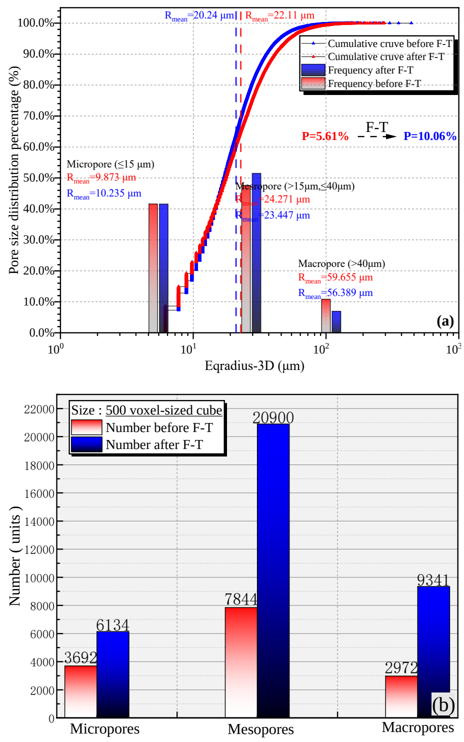

Fig.8 Pore size distribution of turfy soil before and after freeze-thaw by CT (a. percentage, b. number)

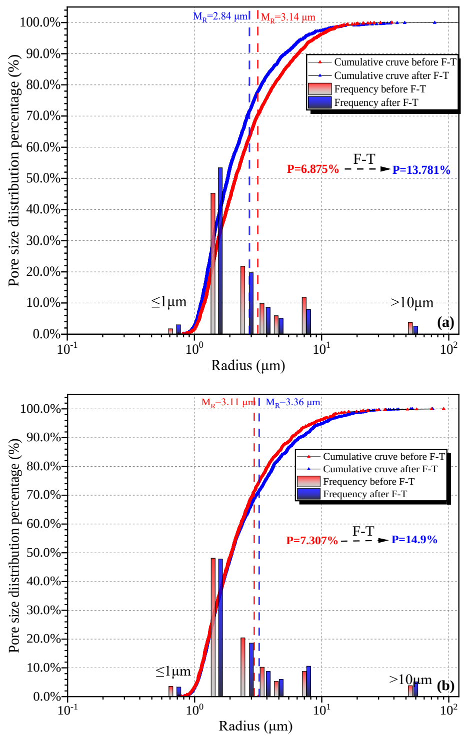

Fig.9 Pore size distribution obtained by SEM (Turfy soil from a. layer 3; b. layer 5)

Fractal dimension and specific surface area ((*S/V*)) are important shape factors to characterize material properties, which can be statistically analyzed by pore identification, as shown in Fig. 10. The fractal dimension characterizes the complexity of the shape and surface roughness, which, can be used as an important basis for hydraulic parameters. After freeze-thaw, the fractal dimension of turfy soil tends to be denser, the inhomogeneity decreases, and the mean value decreases (1.177 to 1.17). This shows that the pore shape complexity of turfy soil tends to be uniform, and the shape complexity decreases. This is consistent with the pore size distribution analysis; the pores tend to be mesoporous after freeze-thaw. The *(S/V)* of mesopores in turfy soil after freeze-thaw slightly decreases, and that of macropores increases, which can be used in pore distribution analysis of the NMR method.

Considering the water-storage pores in turfy soil as cylindrical (*F*=2), combined with Equation (6), the NMR T_2 distribution curve during the freeze-thaw process can be converted into the pore size distribution curve, taking turfy soil from layer 6 as an example shown in Fig. 11. During the freeze-thaw process, the large-sized water storage pores (free water) freeze first. The water in the small-sized pores (capillary water) begins to freeze at -3 ℃. The frozen water is transformed into solid phase ice, forming smaller water storage pores (bound water). This part of water will not freeze at lower temperatures (even lower than -10 ° C), called unfrozen water. During the thawing process, the water in the small-sized water storage pores thaws first, and the main thawing process occurs after 0 ℃. In contrast, the soil's most severe freezing temperature range is -2 ℃ to -3 ℃.

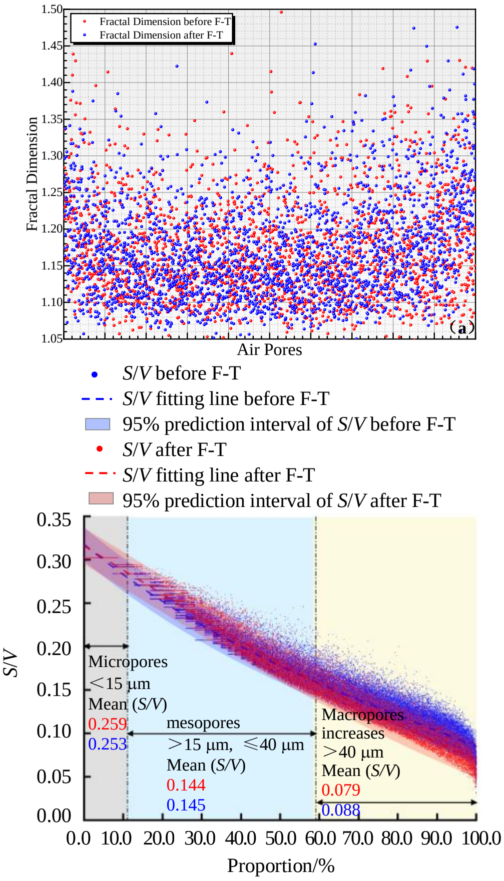

Fig.10 Pore shape factors of turfy soil from layer 5 (a. fractal dimension, b. (S/V))

When the mean radius of each water storage pore at 5 ℃ before and after freeze-thaw is compared, as shown in Table 4, the size of bound water and capillary water pores has increased, consistent with the conclusion that the soil structure tends to be loose. The mean radius of bulk water pores decreased significantly, presumably due to incomplete water thawing or the water boundary enrichment effect of the NMR sample tube.

Table 4 Mean radius of the water-storage pore

	The mean radius of the water-storage pore /μm			
	Bound water	Capillary water	Bulk water	Total
Before F-T	0.167	0.560	27.81	2.010
After F-T	0.176	0.598	5.128	1.024

3.2.3 Connectivity and hydraulic properties

The porosity of the layer 5 turfy soil calculated by Equation (1) is 82.82%, which is less than the sum of the n_{CT} and V_{Oc} derived from the CT segmentation, which is in line with the microstructures of turfy soil concluded in 3.1. The connectivity of each component can be identified by 3D reconstruction, as shown in Fig. 12. About 28.47% of isolated air pores exist. In contrast, the organic matter components of turfy soil are approximately connected, which proves the "matrix" nature of the organic matter components. Changes in the pore characteristics of the soil will affect its internal microstructure and permeability. Based on the connectivity, the permeability, and the pore hydraulic tortuosity, the specimen can be derived by seepage simulation of applying water head. Meanwhile, the hydraulic properties of the soil can also be derived from the connectivity rate, and then a ball-stick model (Fig. 12(b)) is established to show the water storage space and water passage inside the soil.

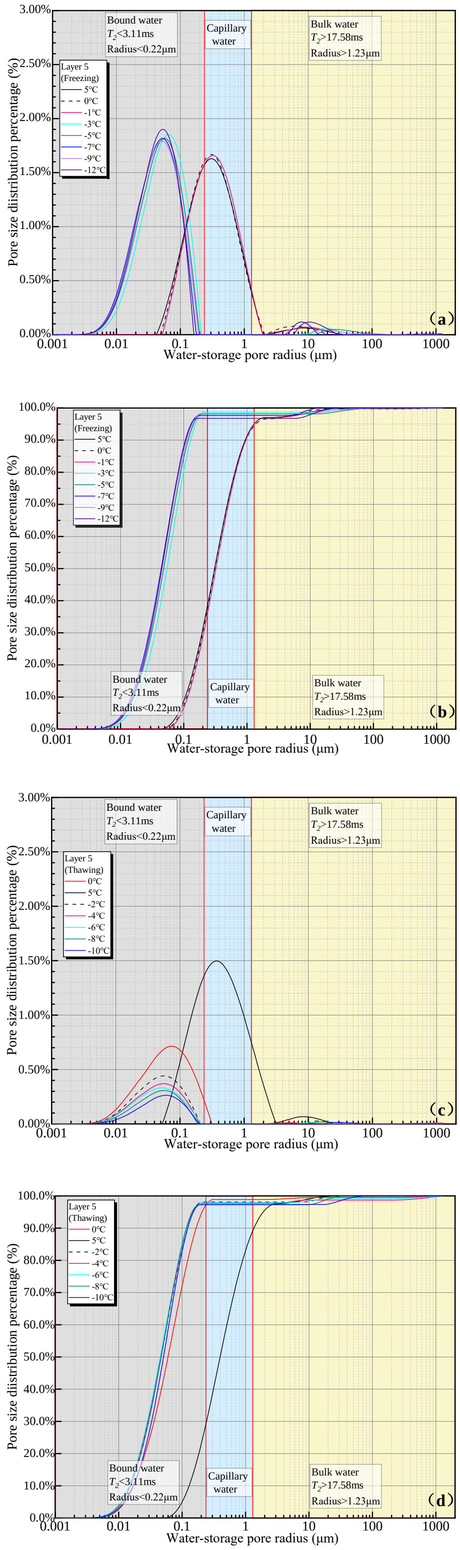

Fig.11 Water-storage pore size distribution during freeze-thaw of turfy soil from layer5(a, c: distribution curve for freezing and thawing process; b, d: cumulative curve)

By establishing a ball-and-stick model of the connected pore network before and after freeze-thaw, the changes in the size and connectivity of the connected pores can be observed visually, as shown in. It can be found that the pore ball-and-stick model becomes denser after freeze-thaw, with an increased number of water passages, enhanced connectivity, and consequently increased permeability. Pore tortuosity is a parameter characterizing the degree of permeability and air permeability of pores in a geotechnical body, which is mainly affected by the geometrical differences between connected pores and is divided into geometrical tortuosity and hydraulic tortuosity. This study focuses on the pore characteristics of the geotechnical body and its seepage properties, so the hydraulic tortuosity is selected, which is the ratio of the actual fluid flow line length in the pore space to the pore space appearance. In this study, the pore tortuosity of turfy soil before freeze-thaw is 2.21, which is in line with the results of Gong's study. The permeability (k_{CT}) is 8.54 μm^2, which is similar to the results (6.37 μm^2-10.37 μm^2 and 6.7 μm^2-7.1 μm^2) from Gong and Yang et al. applying different methods (X-lab and LBM theories)[43; 45].

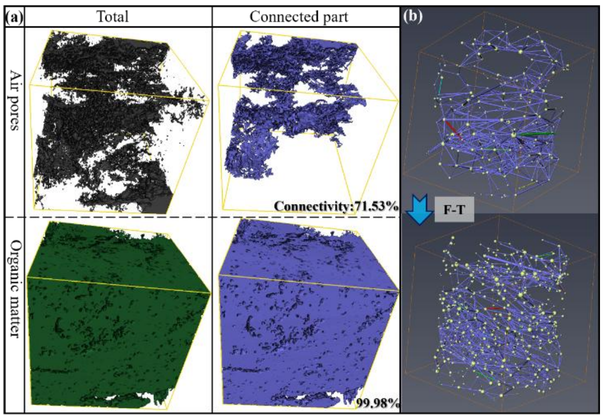

Fig.12 The connectivity (a) of each component and ball-and-stick model (b) of turfy soil

The microstructure, pore characteristics, and seepage properties of turfy soil before and after freeze-thaw are summarized, and the micro-scale changes of soil can be quantitatively analyzed, as shown in Table 5. However, the connectivity rate of air pores decreased after the increase in air pores numbers, and the connectivity rate of organic matter components remained at the level of complete connection. The simulated permeability (k_{CT}) obtained from seepage simulation after CT 3D reconstruction of turfy soil increased to 16.28 μm^2 after freeze-thaw. The quantitative analysis results also show that turfy soil structure tends to be loose, and the comparison results can be used as a reference for the change of microstructures under the freeze-thaw action of permafrost and seasonally frozen soil.

Meanwhile, the permeability coefficient (K_ω) of turfy soil from layer 5 obtained by the variable head permeability test is 3.82E-05cm/s. Thus, the permeability obtained by experiment (k_t) is 5.79μm^2 at 5 ℃ (η=1.52E-03 Pa·s), derived by Equation (3), which is consistent with the permeability simulation results of the above 3D reconstruction. The permeability (k_{NMR}) of turfy soil from layer 5, calculated by the NMR method from Equation (7), is 10.14μm^2 after conversion by Equation(3). The results (k_{CT}, k_t, k_{NMR}) are in the same order of magnitude and relatively close. Thus, the permeability of turfy soil obtained by CT and NMR methods is reliable. Further, the NMR results can be applied to derive the permeability of the soil during the freeze-thaw process as an important parameter for the multi-field coupling numerical model.

Table 5 Quantitative comparison of microstructure and pore characteristics after freeze-thaw

	Before F-T	After F-T
Air pore volume ratio /%	5.61	10.06
Organic matter volume rate /%	92.58	88.45
Volumetric rate of soil particles /%	1.81	1.49
Air pore connectivity /%	71.53	76.27
Organic matter connectivity /%	99.98	99.98
Permeability /μm^2	8.54	16.28
Hydraulic tortuosity	2.21	2.02

3.3 Prediction and verification of permeability coefficient of frozen soil

The permeability coefficient (K) is an important index to describe the migration ability of water in the soil, and it is also an important parameter of the multi-field (thermo-hydro-mechanical) coupling numerical model of frozen soil[46]. The commonly used calculation method of frozen soil permeability coefficient (K_t) generally adopts the most widely used unsaturated soil theory, as shown in Equation (2). In this study, saturation (S) is calculated based on the unfrozen water content, and the unfrozen water is obtained using the parametric model proposed by He et al.[41], which considers the organic matter content and decomposition degree of turfy soil. NMR results can also be applied to predict the permeability coefficient (K_{NMR}) of turfy soil during freeze-thaw, according to Equation (7). As shown in Fig. 13(a), the permeability coefficient of turfy soil from each layer before freeze-thaw obtained by both methods is very close. In contrast, the abnormal result (K_t) of turfy soil from layer 8 is inferred as a test measurement error. There was no significant difference in the permeability coefficient of turfy soil in each layer (mean 1.28E-05 cm/s). Many water channels are formed in the soil by the crisscrossing of plant fiber. Therefore, the permeability coefficient of turfy soil is much higher than that of other common soft soil. Fig. 13(b) illustrates that due to the phase change of water ice, the water channel is blocked by solid ice, and the permeability coefficient of soil decreases sharply by several orders of magnitude in the frozen state (10^{-4}–10^{-12} cm/s). Compared with the K_t calculated by the unsaturated soil theory and the K_{NMR} based on the NMR theory, both predicted values in the initial stage (5°C), and the frozen stable stage (<−3°C) are consistent. This shows that the information on soil water-storage pore characteristics reflected by the NMR method is effective, and the change of permeability of soil during the freeze-thaw process can be obtained accurately.

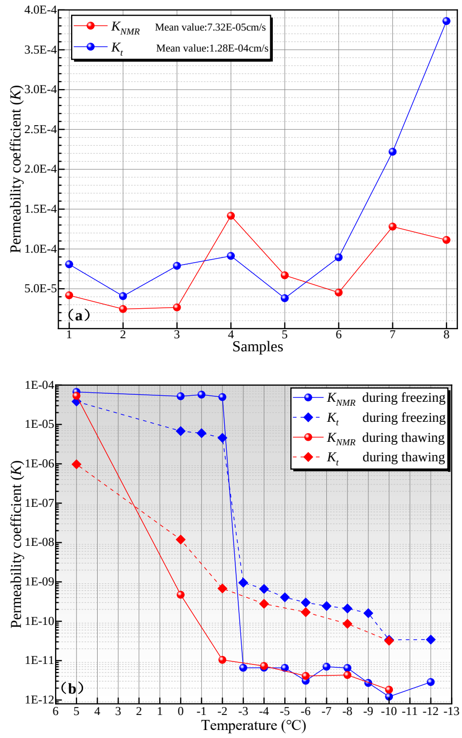

Fig.13 Permeability coefficient (K) of turfy soil obtained by VG model and NMR derivation (a. K of turfy soil from each layer at 5°C, b. K of turfy soil from layer 5 during freeze-thaw)

4 Conclusion

In this study, combined methods, including SEM, CT, and NMR, were used to investigate the microstructure and pore characteristics of high organic matter turfy soil, and the effect of freeze-thaw was revealed. Firstly, the difference between the water-storage pores obtained by theoretical calculation and the air pores obtained by image segmentation is distinguished, and the visual and quantitative expression of the microstructure of turfy soil is given. Secondly, turfy soil's pore size distribution and hydraulic properties were quantitatively characterized. The differences in the properties of turfy soil before and after freeze-thaw were compared, and the influence mechanism was analyzed. Finally, based on NMR theory, the permeability coefficient of turfy soil during the freeze-thaw process was predicted and verified. The following conclusions can be drawn:

(1) Turfy soil has microstructures of organic matter fractions as the matrix, plant fibers as the skeleton, distributed mineral particles, and hollow pores therein. In

turfy soil, the proportion of air pores accounted for 5−7 % and increased to 10−14 % after freeze-thaw. The organic matrix with sponge properties can contain water and conduct water, which forms water storage pores with air pores, accounting for 65−83 % of the proportion.

(2) CT has a better 3D reconstruction ability of samples, while SEM has a higher surface resolution. After the freeze-thaw of turfy soil, new small pores formed, and some of the original pores were connected, which showed that the proportion of mesopores (radius between 2.5 to 15μm) increased and the number of soil pores increased. The mean fractal dimension of the soil decreased from 1.77 to 1.70 after freeze-thaw, reflecting that the pore size of the soil tended to be uniform, and the shape complexity decreased.

(3)The high-connectivity organic matter components, the tubular structure of plant residues, and the through-type air pores distributed along the plant fibers constitute the water channels of turfy soil. The permeability of turfy soil obtained by the variable head test, NMR theory, and 3D reconstruction is consistent, which shows the mean permeability coefficient of turfy soil is 1.28×10^{-5} cm/s cm/s. After freeze-thaw, the air pores connectivity is enhanced, and soil permeability is increased from 8.54μm^2 to 16.28μm^2. Verification by unsaturated soil theory indicates that the permeability coefficient of freezing and thawing turfy soil predicted by the NMR method is effective.

Conclusions and results can be used as the theoretical basis for the study of the microstructure and pore characteristics of soils with high organic matter, high fiber content, and seasonally frozen soil. They also provide the parameter basis for the engineering construction in these soils and for the engineering construction in the turfy soil distribution region.

Reference

[1] MIRAKI H, SHARIATMADARI N, GHADIR P, et al. Clayey soil stabilization using alkali-activated volcanic ash and slag[J]. **Journal of Rock Mechanics and Geotechnical Engineering**, 2022, 14(2): 576-591.

[2] AN R, KONG L, ZHANG X, et al. Effects of dry-wet cycles on three-dimensional pore structure and permeability characteristics of granite residual soil using X-ray micro-computed tomography[J]. **Journal of Rock Mechanics and Geotechnical Engineering**, 2022, 14(3): 851-860.

[3] HUANG Xian-wen, YAO Zhi-shu, CAI Hai-bing, et al. Prediction of thermal conductivity of unsaturated frozen soil based on microstructure remodeling[J]. **Rock and Soil Mechanics**, 2023, 44(1): 193-205.

[4] ZHOU Feng-xi, ZHAO Wen-cang. Estimating unfrozen water content in unsaturated frozen soils based on soil water characteristic curve[J]. **Rock and Soil Mechanics**, 2024, 45(9): 2719-2727.

[5] SUN W J, CUI Y J. Determining the soil-water retention curve using mercury intrusion porosimetry test in consideration of soil volume change[J]. **Journal of Rock Mechanics and Geotechnical Engineering**, 2020, 12(5): 1070-1079.

[6] KIMURA S, NODA S, MINAGAWA H. Experimental investigation of effects of mica content, Fe and pressure on the pore size distribution and permeability of sandy sediment using proton nuclear magnetic resonance[J]. **Engineering Geology**, 2021, 295: 106408.

[7] LI H R, QIAO Y F, HE M C, et al. Effect of water saturation on dynamic behavior of sandstone after wetting-drying cycles[J]. **Engineering Geology**, 2023, 319: 107109.

[8] WANG Qing-yu, TENG Ji-dong, ZHONG Yu, et al. Mesoscale simulation of pore ice formation in saturated frozen soil by using lattice Boltzmann method[J]. **Rock and Soil Mechanics**, 2023, 44(1): 317-326.

[9] KEATING K, WALSH D O, GRUNEWALD E. The effect of magnetic susceptibility and magnetic field strength on porosity estimates determined from low-field nuclear magnetic resonance[J]. **Journal of Applied Geophysics**, 2020, 179: 104096.

[10] KEATING K. A laboratory study to determine the effect of surface area and bead diameter on NMR relaxation rates of glass bead packs[J]. **Near Surface Geophysics**, 2014, 12(2): 243-254.

[11] MÜLLER-PETKE M, DLUGOSCH R, LEHMANN-HORN J, et al. Nuclear magnetic resonance average pore-size estimations outside the fast-diffusion regime[J]. **Geophysics**, 2015, 80(3): 195-206.

[12] YANG J W, CUI Y J, MOKNI N, et al. Investigation into the mercury intrusion porosimetry (MIP) and micro-computed tomography (μCT) methods for determining the pore size distribution of MX80 bentonite pellet[J]. **Acta Geotechnica**, 2024, 19: 85-97.

[13] ZONG Y, YU X, ZHU M, et al. Characterizing soil pore structure using nitrogen adsorption, mercury intrusion porosimetry, and synchrotron-radiation based X-ray computed microtomography techniques[J]. **Journal of Soils and Sediments**, 2015, 15(2): 302-312.

[14] JIA H L, DING S, ZI F, et al. Evolution in sandstone pore structures with freeze-thaw cycling and interpretation of damage mechanisms in saturated porous rocks[J]. **Catena**, 2020, 195: 104915.

[15] SHENG D, ZHANG S, NIU F, et al. A potential new frost heave mechanism in high-speed railway embankments[J]. **Geotechnique**, 2014, 64(2): 144-154.

[16] TENG J D, LIU J L, ZHANG S, et al. Frost heave in coarse-grained soils: experimental evidence and numerical modelling[J]. **Geotechnique**, 2022, 73(12): 1100-1111.

[17] CHANG Wen-zheng, WANG Tian-liang, WANG Lin. Experimental study on mechanical characteristics of mud pumping in railway subgrade under hydrothermal action[J]. **Rock and Soil Mechanics**, 2024, 45(11): 1-11.

[18] NIU C Y, ZHU Z M, ZHOU L, et al. Study on the microscopic damage evolution and dynamic fracture properties of sandstone under freeze-thaw cycles[J]. **Cold Regions Science and Technology**, 2021, 191: 103328.

[19] HUANG S B, YU S L, YE Y H, et al. Pore structure change and physico-mechanical properties deterioration of sandstone suffering freeze-thaw actions[J]. **Construction and Building Materials**, 2022, 330: 127200.

[20] ROONEY E C, BAILEY V L, PATEL K F, et al. Soil pore network response to freeze-thaw cycles in permafrost aggregates[J]. **Geoderma**, 2022, 411: 115674.

[21] LV Y, NIE L, XU K, et al. Study on the difference between Turfy soil and normal peat soil in China[J]. **Applied Mechanics and Materials**, 2012, 105-107: 1551-1554.

[22] NIE L, LV Y, LI M. Influence of organic content and degree of decomposition on the engineering properties of a peat soil in NE China[J]. **Quarterly Journal of Engineering Geology & Hydrogeology**, 2012, 45(4): 435-446.

[23] LÜ Yan. Study on the structural characteristics and model of marsh Turfy soil in the east of Jilin Province[D]. Changchun: Jilin University, 2012: 15-29.

[24] HE Y, XU Y, LV Y, et al. Characterization of thermal conductivity of seasonally frozen turfy soil from Northeastern China[J]. **Bulletin of Engineering Geology and the Environment**, 2022, 81(11): 481.

[25] Ministry of Water Resources of the People's Republic of China. GB/T 50123－2019 Standard for geotechnical testing method[S]. Beijing: China Planning Press, 2019.

[26] CARR H Y, PURCELL E M. Effect of diffusion on free precession in nuclear magnetic resonance experiments[J]. **Physical Review**, 1954, 94(3): 630-638.

[27] MEIBOOM S, GILL D. Modified spin-echo method for measuring nuclear relaxation times[J]. **Review of Scientific Instruments**, 1958, 29(8): 688-691.

[28] SHI Y J, ZHANG L H, MA W, et al. Investigating unfrozen water and its components during freeze-thaw action in loess using a novel NMR technique[J]. **European Journal of Soil Science**, 2022, 73(4): 13262.

[29] VAN GENUCHTEN, TH M. A closed-form equation for predicting the hydraulic conductivity of unsaturated soils[J]. **Soil Science Society of America Journal**, 1980, 44(5): 892-898.

[30] MUALEM, YECHEZKEL. A new model for predicting the hydraulic conductivity of unsaturated porous media[J]. **Water Resources Research**, 1976, 12(3): 513-522.

[31] LU Ning, LIKOS W J. Unsaturated soil mechanics[M]. Beijing: Higher Education Press, 2012.

[32] XU Xue-zu, WANG Jia-cheng, ZHANG Li-xin. Physics of frozen soils[M]. Beijing: Science Press, 2010.

[33] CUI Z D, JIA Y J. Analysis of electron microscope images of soil pore structure for the study of land subsidence in centrifuge model tests of high-rise building groups[J]. **Engineering Geology**, 2013, 164: 107-116.

[34] FAN W H, YANG P, YANG Z H. Freeze-thaw impact on macropore structure of clay by 3D X-ray computed tomography[J]. **Engineering Geology**, 2021, 280: 105921.

[35] TANG Chao-sheng, SHI Bin, WANG Bao-jun. Factors affecting analysis of soil microstructure using SEM[J]. **Chinese Journal of Geotechnical Engineering**, 2008, 30(4) : 560-565.

[36] COATES G R, XIAO L, PRAMMER M G. NMR logging: principles and applications[M]. Houston: Gulf Professional Publishing, 1999: 80-83.

[37] JAEGER F, SHCHEGOLIKHINA A, AS H V, et al. Proton NMR relaxometry as a useful tool to evaluate swelling processes in peat soils[J]. **Open Magnetic Resonance Journal**, 2010, 3(2): 27-45.

[38] JAEGER F, BOWE S, AS H V, et al. Evaluation of 1H NMR relaxometry for the assessment of pore size distribution in soil samples[J]. **European Journal of Soil Science**, 2010, 60(6): 1052-1064.

[39] MEYER M, BUCHMANN C, SCHAUMANN G E. Determination of quantitative pore size distributions of soils with 1H-NMR Relaxometry[J]. **European Journal of Soil Science**, 2015, 69(3): 393-406.

[40] COATES G R, PEVERARO R C A, HARDWICK A, et al. The magnetic resonance imaging log characterized by comparison with petrophysical properties and laboratory core data[C]// SPE Annual Technical Conference and Exhibition. Dallas: [s. n.], 1991: 627–635.

[41] HE Y Y, XU Y, LV Y, et al. Characterization of unfrozen water in highly organic turfy soil during freeze-thaw by nuclear magnetic resonance[J]. **Engineering Geology**, 2023, 312: 106937.

[42] FELDKAMP L, DAVIS L, KRESS J. Practical cone-beam algorithm[J]. **Journal of the Optical Society of America A**, 1984, 1(6): 612-619.

[43] YANG Sheng-tao, LÜ Yan, HE Yuan-yuan, et al. Analysis of pore structure characteristics and seepage simulation of turfy soil based on CT scans[J]. **Journal of Engineering Geology**, 2021, 29(5): 1354-1365.

[44] VINCENT L, SOILLE P. Watersheds in digital spaces: an efficient algorithm based on immersion simulations[J]. **IEEE Transactions on Pattern Analysis and Machine Intelligence**, 1991, 13(6): 583-598.

[45] GONG Lin-xian. Study on meso-structure and mechanical characteristics of turfy soil in seasonally frozen area[D]. Changchun: Jilin University, 2020: 65-82.

[46] ZHELNIN M, KOSTINA A, PROKHOROV A, et al. Coupled thermo-hydro-mechanical modeling of frost heave and water migration during artificial freezing of soils for mineshaft sinking[J]. **Journal of Rock Mechanics and Geotechnical Engineering**, 2022, 14(2): 537-559.